Flat-end Cutter Accessibility Determination in 5-axis Milling of Sculptured Surfaces

L. L. Li[1] and Y. F. Zhang[1*]

[1]National University of Singapore, *mpezyf@nus.edu.sg

ABSTRACT

In this paper, a point-based method is developed to check whether a flat-end cutter is able to finish the entire sculptured surface without any interference in 5-axis milling. In order to reduce the heavy computation load, the surface is firstly decomposed into interference-prone and interference-free regions by considering the local surface geometry and the cutter's geometry. At the point within the interference-prone regions, a comprehensive search algorithm has been developed to find the accessible posture range for a given cutter in terms of the tilting and rotational angles. The constraints considered in cutter accessibility determination include machine's axis limit, local-gouging, rear-gouging, and global-collision. Examples are given to show the validity, efficacy and robustness of the developed methods.

Keywords: cutter selection; local and rear-gouging; global-collision, accessible posture range, 5-axis milling.

1. INTRODUCTION

Five-axis machining of free-form surfaces has one major advantage over three-axis machining, i.e., a greater degree of flexibility in positioning the cutting tool relative to the surface. However, because of the two additional revolute axes, the complication in process planning steps, such as selecting the optimal cutter and generating interference-free tool-paths, is also brought with the added cutter orientation control and movement of the cutter.

The process planning tasks for 5-axis machining (finish cut) include cutter selection and tool-path generation. In the literature of process planning for 5-axis machining, most of the previous effort focuses on developing automated methods to generate an interference-free tool-path for a given designed surface and cutter [3, 7]. There is limited reported work on cutter selection in 5-axis machining. Lee and Chang [2] proposed a cutter selection algorithm of flat-end cutter by calculating the maximum effective cutting radius at every sampled point. At each sampled point, the feasibility cone is firstly constructed to obtain the feasible range of the incline angle and tilt angle. The feasible angle range is then sampled and evaluated to find the effective cutting radius range. A feasible cutter is identified if at every sampled point, the radius of curvature is larger than the effective cutting radius. Jensen et al. [1] developed a cutter selection algorithm for fillet-end cutters based on curvature matching machining, in which local-gouging, rear-gouging, and global-collision are considered. The algorithm is of trial-and-error in nature. It starts with the largest cutter in a tool database. Beginning from the first point in the sampled data set and the feeding direction, tool interference detection and correction algorithm is applied to find an interference-free orientation within the machine limit. If at one specific point no such orientation is available, another cutter with larger minor radius or smaller major radius is selected to repeat the checking algorithm. To a certain extent, this method still follows the tool-path generation approach. So far, there is no effective reported method that can determine whether a cutter can finish a given surface before tool-path generation.

The cutter selection problem can be defined as "given a designed surface, a 5-axis machine, and a set of cutters, find the best cutter that can traverse the entire surface without interference". Here, *interference* refers to local-gouging, rear-gouging, and global-collision. Cutter selection can be considered as a two-phase decision-making process. The first task is to determine those suitable cutters, from the cutter set, that can finish the entire surface. The second task is to choose the best cutter from the suitable cutters according to some optimization criteria. This paper focuses on solving the problems in the first task, which is essentially to check whether a given cutter can finish the entire surface. To be more specific, at a point on the surface, if the cutter has a posture that causes no interference, the cutter is said to be accessible to this point. If the cutter is accessible to any point on the surface, the cutter is said to be feasible. In this paper, a two-phase approach is proposed to check the suitability of the cutter. In phase-I, the part

surface is firstly sampled to obtain a set of points. These points are then divided into two groups, the interference-prone and interference-free, by analyzing the geometric properties of the points and the cutter. In phase-II, three algorithms are developed to check the accessibility of a cutter to an interference-prone point with respect to local-gouging, rear-gouging, and global-collision.

In machining process planning, cutter selection is typically carried out before tool-path generation. The method proposed in this paper deals with the problem by checking the cutter accessibility without considering the feeding direction. In order to shorten the computation time, a new sampling strategy is developed to divide the entire surface into interference-prone and interference-free regions. The accessibility checking will be carried out only within the interference-prone regions.

Section 2 describes a surface decomposition algorithm that effectively divides the entire surface into interference-prone and interference-free regions. In Section 3, the point-based cutter accessibility checking algorithm is presented. Two application examples are presented to validate the developed algorithm in Section 4. Finally, conclusion remarks are given in Section 5.

2. SURFACE DECOMPOSITION FOR CUTTER SELECTION

NURBS (Non-Uniform Rational *B*-Spline) representation is widely used for sculptured surfaces in industry [5]. In this paper, a machined surface is described by a set of NURBS patches $\mathbf{S}_i(u,v)$ with C^2 continuity. A flat-end cutter is described by its radius (R) and length (L). Since a sculptured surface can be represented as a set of surface patches that are trimmed by one or more curves, the following discussion will focus on a single NURBS patch without losing generality.

2.1 Local surface geometry property

Surface properties, such as unit normal vector and curvature, are well defined in the literature [4]. For a specific point on the surface patch $\mathbf{S}(u,v)$, there exist the maximum ($\kappa_{\max}$) and minimum ($\kappa_{\min}$) normal curvature values, also called the principal curvatures, for all the curves passing through this point. This kind of curvature property can be represented with two variables: Gaussian curvature (K) and Mean curvatures (H):

$$K = \kappa_{\max} \times \kappa_{\min} = \frac{LN - M^2}{EG - F^2} \tag{1}$$

$$H = \frac{1}{2}(\kappa_{\max} + \kappa_{\min}) = \frac{EN + GL\text{-}2FM}{2(EG - F^2)} \tag{2}$$

Where *E, F, G* and *L, M, N* are the magnitudes of the first and second fundamental forms at the specific point, respectively. Based on the values of *K* and *H*, the local surface shape around the point can be divided into three categories: convex, concave and saddle [5]:

(1) $K \geq 0$ and $H \leq 0$: $\kappa_{\max}$ and $\kappa_{\min}$ are smaller than or equal to zero, local surface is convex.
(2) $K \geq 0$ and $H > 0$: $\kappa_{\max}$ and $\kappa_{\min}$ are greater than or equal to zero, local surface is concave.
(3) $K < 0$: $\kappa_{\max}$ and $\kappa_{\min}$ have different signs, local surface is saddle.

In theory, a surface $\mathbf{S}(u,v)$ can be decomposed by the curves on which $K(u,v)=0$. However, $K(u,v)$ is a complicated expression of *u* and *v* for a NURBS surface patch, and, it is very difficult to solve this equation analytically. For implementation, a numerical method seems more feasible. Here, the surface patch is first uniformly sampled in *u* and *v* directions to obtain a set of grid points. At each grid point, the Gaussian curvature and Mean curvature are calculated. Next, the points with concave and saddle local property are identified. The neighboring concave and saddle points are grouped together to form concave regions and saddle regions, respectively. The remaining points form convex regions. The boundary points are linked up to form their respective boundaries. Up to this point, the surface subdivision based on local surface shape is completed. An example of the surface subdivision is shown in Fig. 1a.

The points within the concave regions and saddle regions are interference-prone. For points within the convex regions, local-gouging can be effectively ruled out. However, rear-gouging and global-collision may still occur, especially at the points that are close to the boundary. An interesting observation is that, starting from the centre of a convex region, the closer a point is to the boundary, the more interference-prone (in particular rear-gouging) the point is. It is therefore possible to identify a portion of the convex region that is free of rear-gouging and global-collision, thus further reducing the checking area.

(a) Surface subdivision based on local surface shape

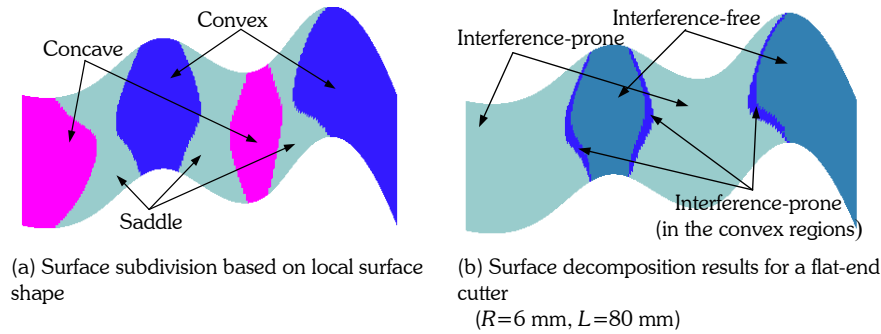(b) Surface decomposition results for a flat-end cutter
(R=6 mm, L=80 mm)

Fig. 1. An example of identifying interference-prone and interference-free regions

2.2 Identifying the interference-free area from a convex region

As shown in Fig. 2a, when a flat-end cutter (R, L) is positioned at a point on a surface, at which the cutting edge is in contact with the surface. This point is called the cutter-contact (CC) point. Rear-gouging occurs if part of the cutter bottom surface is underneath the part surface. Global-collision occurs if the distance between the cutter axis and the surface is less than R within the range of cutter length (L). Hence, the detection of rear-gouging and global-collision is in fact a distance-evaluation problem. However, a numerical method is the only solution to solve this problem, which is very time consuming. At the same time, since the feeding direction is not fixed, the cutter could approach the point from any direction. If we position the cutter along a fixed direction, say the normal direction of the point on the surface, the envelop surface of the cutter in all possible positions effectively forms a cylinder with a radius of $2R$ and length of L (see Fig. 2b). We call this cylinder a *dummy cutter* of the given cutter. It can be seen that the volume occupied by the given cutter at all possible feeding directions towards the point is inside the volume occupied by its dummy cutter. Therefore, we can check the accessibility of a given cutter (R, L) at a point along the normal direction of the point by checking the accessibility of a cutter ($2R, L$) with its bottom centre at the point and its axis along the normal direction of the point. If the dummy cutter does not have any interference at the point, the given cutter does not either. By using the dummy cutter, we effectively simplify the accessibility checking problem for a given cutter in non-fixed feed direction. It is worth mentioning that this simplification process uses a tighter criterion to check the accessibility of a point to a cutter by positioning the cutter along the normal direction of the point only. Although some interference-free points in the convex region may be treated as interference-prone, it will not have any negative effect at the later stage since we are only interested in identifying the interference-free regions quickly at this stage.

(a)   (b)   (c)
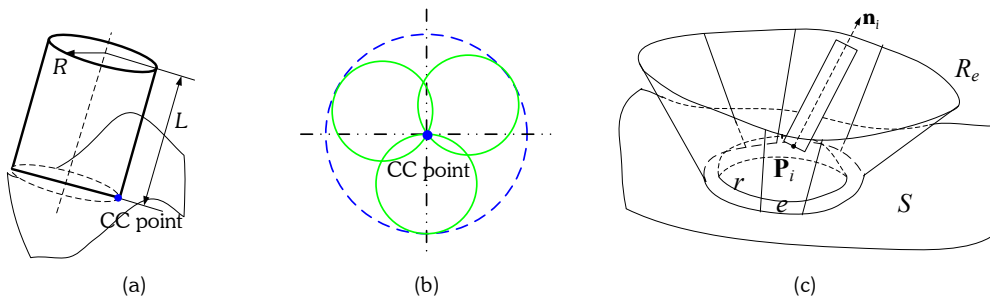
Fig. 2. The flat-end cutter and its dummy cutter for interference checking on a convex regions r

Now, we proceed to identify the interference-free portion of a convex region by using the dummy cutter. A general case for this problem is presented in Fig. 2c, where r is a single convex region to be checked on the part surface S. e represents its boundary and Xr represents all the other regions on S except r.

Theorem 1: Given any point on r, a flat-end cutter is positioned with its bottom centre at the point and its axis along the normal direction at the point. If the cutter is interference-free (rear-gouging and global-collision) at any point on e, the cutter is interference-free at any point on r.

Proof:
Since the cutter is positioned with its axis along the normal direction of the point on *r* and every point on *r* is convex, the cutter will not have any interference with any point on *r*. Now, referring to Fig. 2c, R_e is the surface consisting of *r* and the enveloping surface formed by the cutter bottom plane and shaft outside surface undergoing the movement (the cutter axis along the normal direction of the point and the bottom centre at the point) along the boundary curve *e*. Since the cutter is interference-free on *e*, R_e will have no interference with any of the remaining surface patches, namely *Xr*. When the cutter is placed at any point $\mathbf{P}_i$ within *r*, it could be proved [6] that its axis (normal at point $\mathbf{P}_i$) is within those at points on *e*. The cutter bottom plane at $\mathbf{P}_i$ is then above *r* and its cylindrical surface is inside R_e. Therefore, the cutter is completely inside R_e and will not have any interference with any of the remaining surface patches, namely *Xr*. Therefore, at any point on *r*, the cutter is interference-free.

The above theorem can simplify the checking procedure for flat-end cutter by converting the surface checking problem into a curve checking problem. The task of identifying the interference-free portion from a convex region is converted to identifying the largest boundary (from the convex region) on which the dummy cutter is interference-free. The detailed algorithm is given as follows:

Input: (1) *A part surface represented by a set of trimmed NURBS patches S_i with C^2 continuity.*
(2) *A given flat-end cutter (R, L).*

Output: *A set of interference-free points $\{S_{i\text{-}free}\}$ and a set of interference-prone points $\{S_{i\text{-}prone}\}$*
Begin
    (1) Sample the trimmed surfaces to a set of grid points. Identify the convex/concave/saddle regions, each with a set of points and its boundary. Put the concave and saddle points into $\{S_{i\text{-}prone}\}$.
    (2) Pick a convex region *r* and place its boundary points into a point set $\{e\}$ and other points in $\{\mathbf{P}_i\}$. *Xr* represents all the other surface regions except *r*. Create an empty boundary point set $\{e_{i\text{-}free}\}$ for its interference-free portion. Pick one point from the point set $\{e\}$.
    (3) Place the dummy cutter (2R, L) with its bottom centre at the point and its axis in the normal direction of the point. (a) check whether the cutter's posture is within the machine axis limit, (b) calculate the distance between the cutter bottom plane and the sampled points on *Xr* for gouging detection and (c) calculate the distance between the cutter axis and the sampled points on *Xr* for collision detection.
    (4) If this point is free of interference, place it into $\{e_{i\text{-}free}\}$, and find the next point in $\{e\}$, go back to (3). Otherwise, place the point into $\{S_{i\text{-}prone}\}$ and find the nearest point of the current point in $\{\mathbf{P}_i\}$, go back to (3). If no more points are left in $\{e\}$, put $\{e_{i\text{-}free}\}$ and the remaining points in $\{\mathbf{P}_i\}$ into $\{S_{i\text{-}free}\}$. Go to (5).
    (5) If all the convex regions are traced, stop. Otherwise, Go back to (2)
End

The above algorithm has been implemented by using C++ and OpenGL. For the example shown in Fig. 1a, 201×201 points are obtained by sampling the surface uniformly along *u* and *v*, respectively. As shown in Fig. 1a, 43.2% of the points are determined as convex. By using a flat-end cutter (*R*=6 mm, *L*=80 mm), 86.9% of the convex points were further classified as interference-free points, as shown in Fig. 1b. The concave and saddle points are treated as interference-prone and part of the two convex regions (near the boundary) is identified as interference-prone. In summary, about 37.5% of the sampled points were identified as interference-free which is excluded from further checking in cutter selection, thus resulting in significant savings in terms of computation.

3. POINT-BASED CUTTER ACCESSIBILITY CHECKING
There are four attributes to a cutter's accessibility to a point on the surface: machine axis limit, local-gouging, rear-gouging, and global-collision. In this section, the algorithms to check a given cutter's accessibility in terms of the four attributes are introduced. Based on the surface decomposition results, the checking is carried out only at the interference-prone points (local-gouging will not be checked at the convex points). The objective is to check, at a point, whether there exists a posture at which the cutter is interference-free. Given a point, we firstly identify the accessible posture range of the cutter based on each attribute. If there is no accessible posture for an attribute, search is stopped and the cutter is labeled as non-accessible. The common posture range among the four accessible posture ranges is then identified and if the common range exists, the cutter is accessible at the point.

Before the algorithms are described, two coordinate frames are firstly introduced: local frame and tool frame. Local frame is defined according to the surface geometry at the point of interest $\mathbf{P}_c$. As shown in Fig. 3a, the local frame ($\mathbf{X}_L$ –$\mathbf{Y}_L$ –$\mathbf{Z}_L$) originates at $\mathbf{P}_c$ with $\mathbf{Z}_L$ -axis along the normal vector, $\mathbf{X}_L$ -axis along the surface maximum

principal direction, and $\mathbf{Y}_L$ -axis along the surface minimum principal direction. A cutter's orientation is defined by an angle pair (λ, θ) meaning that the cutter's axis inclines with λ about $\mathbf{Y}_L$-axis and rotates a θ about $\mathbf{Z}_L$-axis, where $0° \le \lambda \le 90°$ and $0° \le \theta \le 360°$. Tool frame ($\mathbf{X}_T$ –$\mathbf{Y}_T$ –$\mathbf{Z}_T$) is defined with its origin at the cutter bottom centre while its $\mathbf{Z}_T$ -axis along the cutter axis direction and its $\mathbf{X}_T$ -axis towards $\mathbf{P}_c$. $\mathbf{Y}_T$ -axis is defined by $\mathbf{Y}_T = \mathbf{Z}_T \times \mathbf{X}_T$.

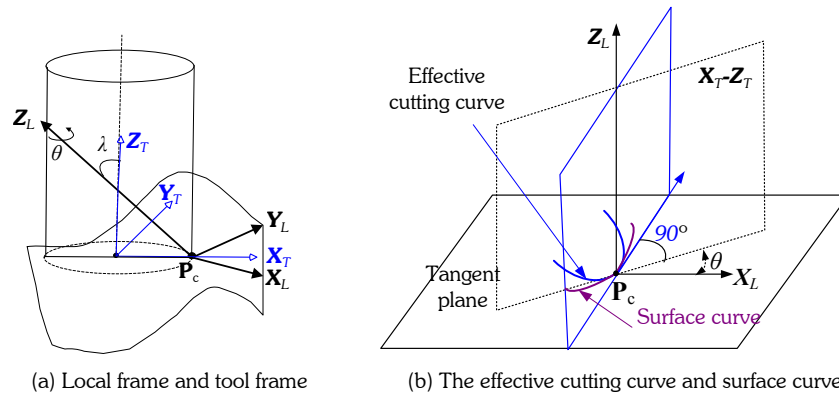| (a) Local frame and tool frame | (b) The effective cutting curve and surface curve |

Fig. 3. The cutter at $\mathbf{P}_c$ in the local frame and tool frame

In the following sections, the algorithms to obtain the accessible posture range (λ, θ) for a given cutter, if such a range exists, are introduced. Among the 4 attributes, identifying the accessible range based on machine limit is rather straightforward [7], which is not to be covered here.

3.1 Cutter posture range for local-gouging avoidance

Local-gouging occurs when the curvature of cutter's cutting edge is less than that of curve on part surface at the point of interest such that the cutter cuts excess material. Therefore, given a posture (λ, θ) of the cutter, the corresponding curvatures in normal direction at the CC point need to be compared to ensure the prevention of local-gouging. At the CC point, the curvature of the effective cutting curve can be expressed as [2]:

$$\kappa_t = \frac{\sin \lambda}{R} \tag{3}$$

According to Euler's formula [4], as shown in Fig. 4b, the normal curvature of the curve at the CC point ($\mathbf{P}_c$) along the direction of the effective cutting curve (normal to $\mathbf{X}_T$ direction) is given as,

$$\kappa_s = \kappa_{max} \cos^2(\theta + \pi/2) + \kappa_{min} \sin^2(\theta + \pi/2) \tag{4}$$

To make sure that the cutter is free of local-gouging at this point, we must have κ_t- κ_s > 0. Therefore, we have,

$$\sin \lambda > R(\kappa_{max} \sin^2 \theta + \kappa_{min} \cos^2 \theta) \tag{5}$$

Given a θ, the minimum values of $\lambda_{\theta\text{-}lg}$, if there is any, can be obtained from Eq. (5) and the accessible range is therefore [$\lambda_{\theta\text{-}lg}$, 90°].

3.2 Cutter posture range for rear-gouging avoidance

For a given θ, we now need to identify a posture range [θ, ($\lambda_{\theta\text{-}rg1}$, $\lambda_{\theta\text{-}rg2}$)] such that cutter bottom surface does not protrude into the part surface. To conduct this search, we first identify all the candidate points on the part surface that have the possibility of causing rear-gouging, thus minimizing the search time. For each candidate point $\mathbf{P}_i|i=1$, n, where n is the total number of candidate points, the accessible range ($\lambda_{\theta\text{-}rg1\text{-}i}$, $\lambda_{\theta\text{-}rg2\text{-}i}$) is then obtained. The common range of all the ($\lambda_{\theta\text{-}rg1\text{-}i}$, $\lambda_{\theta\text{-}rg2\text{-}i}$) $|i=1$, n, is taken as the ($\lambda_{\theta\text{-}rg1}$, $\lambda_{\theta\text{-}rg2}$).

Referring to Fig. 4a, it can be easily shown that, for any point $\mathbf{P}_{tk}$ on the cutter bottom surface, the distance from CC point $\mathbf{P}_c$ | $\mathbf{P}_c\mathbf{P}_{tk}| \le 2R$. Thus the candidate points on the part surface for rear-gouging check should be within a distance range of $2R$ from $\mathbf{P}_c$. In addition, only those points on the surface that is above the tangent plane are possible to rear-gouging. Therefore, a candidate point, $\mathbf{P}(x_T, y_T, z_T)$, must satisfy | $\mathbf{P}_c\mathbf{P}$ | $\le 2R$ and $\mathbf{P}_c\mathbf{P} \cdot \mathbf{Z}_L > 0$.

Now, we show under what condition that a rear-gouging prone point, **P**, causes rear-gouging. As shown in Fig. 4a, if **P** is above cutter bottom surface, rear-gouging occurs. If we increase λ by rotating the cutter about axis $\mathbf{Y'}_T$, **P** tends to move towards underneath the cutter surface. Therefore, we need to find the minimum λ such that **P** is on the cutter outer surface at position **P'** (Fig. 4b).

(a) Gouging-prone **P** (x_T, y_T, z_T) and the cutter   (b) Tilting angle $\Delta\lambda$ for free rear-gouging of **P**

Fig. 4. Identifying cutter posture range for rear-gouging avoidance

Given a candidate point $\mathbf{P}(x_T, y_T, z_T)$, we start with the cutter posture at $\lambda = 0$. As illustrated in Fig. 4b, if **P** is below the cutter bottom surface, the accessible posture range, in terms of λ, is [0, 90°]. Otherwise, we have to adjust angle λ about axis $\mathbf{Y'}_T$ such that **P** will reach the cutter bottom surface at a corresponding point **P'**. The increment $\Delta\lambda$ is calculated as:

$$\Delta\lambda = \sin^{-1}\left(\frac{z_T}{d}\right) = \sin^{-1}\left(\frac{z_T}{\sqrt{(R - x_T)^2 + z_T^2}}\right) \tag{6}$$

Where d, distance between **P** and axis $\mathbf{Y'}_T$, $R - \sqrt{R^2 - y_T^2} < d < R + \sqrt{R^2 - y_T^2}$ for the rear-gouging occurring point.

Since the initial λ is set as 0, the minimum inclining angle λ for the cutter to avoid rear-gouging at point **P** is $\Delta\lambda$ and the accessible posture range, in terms of λ, for the cutter at **P** is [$\Delta\lambda$, 90°], if $\Delta\lambda \leq 90°$. If $\Delta\lambda$ is outside [0, 90°], it means that at θ, rear-gouging cannot be avoided. θ needs to be increased and the search restarts from local-gouging avoidance. Using this method, we can identify the accessible posture ranges for rear-gouging avoidance, at θ, for all the rear-gouging candidate points as $\Delta\lambda_i | i=1, n$. The overall accessible posture range for free of rear-gouging is [θ, ($\lambda_{\theta\text{-}rg}$, 90°)], where $\lambda_{\theta\text{-}rg} = \max\{\Delta\lambda_i | i=1, n\}$.

3.3 Cutter posture range for global-collision avoidance

We now proceed to find a posture range [θ, ($\lambda_{\theta\text{-}gc1}$, $\lambda_{\theta\text{-}gc2}$)] such that the cutter shaft does not intersect with the part surface. In theory, given a posture, a point collides with the cutter if it falls "inside" the cutter, in which the cutter length needs to be considered. Here, we consider that the point collides with the cutter if the distance between the point and the cutter axis is less the R, i.e., we assume the length of the cutter infinite. This may help to cover the constraints imposed by the cutter's holder, which is not considered here. However, the constraints of the cutter's holder can be easily incorporated into our collision-avoidance algorithm if the geometry of the holder is given. Like the search procedure for rear-gouging, we first identify the candidate points on the part surface that have the possibility of causing global-collision, thus minimizing the search time. For each global-collision candidate point $\mathbf{P}_i | i=1, n$, where n is the total number of candidate points, the accessible range ($\lambda_{\theta\text{-}gc1\text{-}i}$, $\lambda_{\theta\text{-}gc2\text{-}i}$) is then obtained. The common range of all the ($\lambda_{\theta\text{-}gc1\text{-}i}$, $\lambda_{\theta\text{-}gc2\text{-}i}$) $|i=1, n$, is taken as the ($\lambda_{\theta\text{-}gc1}$, $\lambda_{\theta\text{-}gc2}$).

Referring to Fig. 5a, it can be seen that in the vicinity of the point $\mathbf{P}_c$, those surface points that "face" the cutter have the possibility to interfere with the cutter shaft. These surface points, such as $\mathbf{P}_3$ and $\mathbf{P}_4$, are identified as collision-prone candidates for analysis. The normal vector $\mathbf{n}_i$ at one specific surface point $\mathbf{P}_i$ can be utilized to determine whether it "faces" the cutter or not, i.e., if $\mathbf{n}_i \cdot \mathbf{P}_c\mathbf{P}_i < 0$, $\mathbf{P}_i$ is "facing" the cutter. In Fig. 5a, $\mathbf{P}_3$ and $\mathbf{P}_4$ are determined as "facing" the cutter and labeled as collision-prone points, while $\mathbf{P}_1$ and $\mathbf{P}_2$ are collision-free points. On the other hand, y_T must be within the range of $-R \leq y_T \leq R$ if it is global-collision prone.

Now, we show how to find the collision-free posture range for a global-collision prone point, $\mathbf{P}(x_T, y_T, z_T)$. We firstly use a plane $y=y_T$ to section the cutter surface (at $\lambda=0$), a section curve is produced as shown in Fig. 5b. The radius of the section curve is $r = \sqrt{R^2 - y_T^2}$. In rear-gouging avoidance, we know that if a rear-gouging prone point does not cause gouging at $\lambda=0$, its posture range, in terms of λ, is [0, 90°]. Otherwise, we need to find the minimum $\Delta\lambda$ that leads to the avoidance of rear-gouging. In global-collision avoidance, however, the posture range for every collision prone point is needed to be found even it does not collide with the cutter at $\lambda=0$. For example, referring to Fig. 5b, if a point causes collision (e.g., $\mathbf{P}$ on the left), i.e., it is inside the section curve (above the cutter bottom portion), we need to find the minimum $\Delta\lambda$ the cutter rotates clockwise to avoid the collision. In this case, the posture range for free of global-collision is [$\Delta\lambda$, 90°]. If the point does not cause collision (e.g., $\mathbf{P}$ on the right), we need to find the minimum $\Delta\lambda$ the cutter rotates clockwise such that the point touches the cutter shaft. In this case, the posture range for free of global-collision is [0, $\Delta\lambda$]. The relative positional relationship between $\mathbf{P}$ and the section curve can be categorized into five cases and the methods that handle the different cases are given as follows:

(1) $z_T < r_f$, $\mathbf{P}$ is collision-free and its accessible posture range is [0, 90°].

(2) $x_T < -r$, and $\mathbf{n} \cdot \mathbf{X}_T > 0$ ($z_T \geq r_f$), $\mathbf{P}$ is collision-free and its accessible posture range is [0, 90°].

(3) $x_T \geq -r$, and $\mathbf{n} \cdot \mathbf{X}_T > 0$ ($z_T \geq r_f$), global-collision exists. The minimum $\Delta\lambda$ that the cutter rotates clockwise to avoid global-collision is $\cos^{-1}\dfrac{R - x_T}{d} - \cos^{-1}\dfrac{R + \sqrt{R^2 - y_T^2}}{d}$. Where d is the distance from $\mathbf{P}$ to $\mathbf{Y'}_T$. The posture range is [$\Delta\lambda$, 90°].

(4) $x_T < r$ and $\mathbf{n} \cdot \mathbf{X}_T < 0$ ($z_T \geq r_f$), global-collision exists. The accessible posture range is NULL.

(5) $x_T \geq r$, and $\mathbf{n} \cdot \mathbf{X}_T < 0$ ($z_T \geq r_f$), $\mathbf{P}$ is collision-free. The minimum $\Delta\lambda$ that the cutter rotates clockwise to cause global-collision is $\cos^{-1}\dfrac{R - x_T}{d} - \cos^{-1}\dfrac{R - \sqrt{R^2 - y_T^2}}{d}$. The posture range is [0, $\Delta\lambda$].

Using the above method, the posture ranges for all global-collision prone points can be obtained as ($\lambda_{\theta\text{-}gc1\text{-}i}$, $\lambda_{\theta\text{-}gc2\text{-}i}$) $|i=1, n$. The overall accessible posture range for free of global-collision is [θ, ($\lambda_{\theta\text{-}gc1}$, $\lambda_{\theta\text{-}gc2}$)], where $\lambda_{\theta\text{-}gc1}$ = max{$\lambda_{\theta\text{-}gc1\text{-}i}$, $|i=1, n$} and $\lambda_{\theta\text{-}gc2}$ = min{$\lambda_{\theta\text{-}gc2\text{-}i}$, $|i=1, n$}. If $\lambda_{\theta\text{-}gc1} > \lambda_{\theta\text{-}gc2}$, it means that the cutter is not accessible at this θ. θ needs to be increased and the search restarts from local-gouging avoidance.

(a) Collision-prone and collision-free points   (b) Section curve on cutter at $y=y_T$
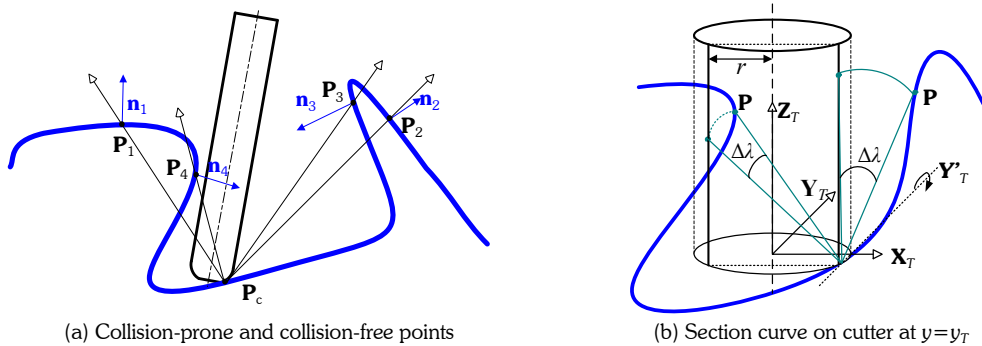
Fig. 5. Identifying cutter posture range for global-collision avoidance

3.4 The overall search algorithm

For an interference-prone point on the part surface, the three methods introduced in Sections 3.1, 3.2, and 3.3 can be used to find [θ, ($\lambda_{\theta\text{-}lg}$, 90°)], [$\theta$, ($\lambda_{\theta\text{-}rg}$, 90°)], and [$\theta$, ($\lambda_{\theta\text{-}gc1}$, $\lambda_{\theta\text{-}gc2}$)], representing the accessible posture ranges for the avoidance of local-gouging, rear-gouging, and global-collision, respectively. If a common range among these three ranges is available, the cutter is accessible to the point. We therefore combine the three methods into an overall search algorithm. It is worth noting that in the above algorithms, we assume the minimum and maximum values of λ as 0° and 90°, respectively. In practice, this can be generalized by using $\lambda_{\min}$ and $\lambda_{\max}$ instead. Similarly, the minimum and maximum values of θ are $\theta_{\min}$ and $\theta_{\max}$, respectively. The algorithm is described as follows:

Algorithm: Finding the accessible posture range of a cutter at a CC point P

Input: (a) All the points on the surface $\{\mathbf{P}_k, k = 1, 2, ..., K\}$ except the CC point $\mathbf{P}$
(b) A flat-end cutter (R, L)
(c) Titling angle range $[\lambda_{min}, \lambda_{max}]$, orientation angle range $[\theta_{min}, \theta_{max}]$

Output: The accessibility of the cutter at $\mathbf{P}$

(1)   Uniformly sample $[\theta_{min}, \theta_{max}]$ into $(n+1)$ angles, set $i = 0$.

(2)   IF $i \leq n$, $\theta_i = \theta_{min} + (\theta_{max} - \theta_{min})(i/n)$; otherwise, go to (7).

(3)   Find the local-gouging free posture range $[\theta_i, (\lambda_{\theta-lg}, \lambda_{max})]$, using the method introduced in Section 3.1. If such a posture range does not exist, $i = i + 1$, go to (2).

(4)   Find the rear-gouging free posture ranges, from $(\lambda_{\theta-lg}, \lambda_{max})$, for $\{\mathbf{P}_k, k = 1, 2, ..., K\}$. The common posture range is taken as $[\theta_i, (\lambda_{\theta-rg}, \lambda_{max})]$, note that $\lambda_{\theta-rg} \geq \lambda_{\theta-lg}$. If such a posture range does not exist, $i = i + 1$, go to (2).

(5)   Find the global-collision free posture ranges, from $(\lambda_{\theta-rg}, \lambda_{max})$, for $\{\mathbf{P}_k, k = 1, 2, ..., K\}$. The common posture range is taken as $[\theta_i, (\lambda_{\theta-gc1}, \lambda_{\theta-gc2})]$, note that $\lambda_{\theta-gc1} \geq \lambda_{\theta-rg}$ and $\lambda_{\theta-gc2} \leq \lambda_{max}$. If such a posture range does not exist, $i = i + 1$, go to (2).

(6)   Output "the cutter is accessible at $\mathbf{P}$". Stop.

(7)   Output "the cutter is not accessible at $\mathbf{P}$". Stop.

It can be seen that the algorithm is, to a large extent, numerical in nature, except that the method to find the accessible range for the avoidance of local-gouging is analytical. Therefore, the computation could be heavy, although some measures are taken to find the rear-gouging prone points and global-collision prone points. Furthermore, the search for the accessible posture range considers only geometric concerns. Some technical concerns, such as the preferable tilting and orientation ranges, also need to be taken into consideration in cutter selection. This can be incorporated by specifying $[\lambda_{min}, \lambda_{max}]$ and $[\theta_{min}, \theta_{max}]$ before the search starts.

4. APPLICATION EXAMPLES

The aforementioned algorithm has been implemented in VC++ and OpenGL environment. In this section, two examples are shown to validate the proposed methodology. In the first example, a simple composite surface shown in Fig. 6 is employed, which consists of two planar patches with 120° angle, and a 60°-cylindrical patch ($R_c = 5$ mm) connecting the former two patches. The surface is symmetric about the bottom line of the cylinder. It was chosen because the accessible posture range of a cutter at any point can be obtained by analytical means. Therefore, the results obtained by using the developed algorithm can be compared to the exact results. The cutter employed has the following parameters: $R = 8$ mm and $L = 90$ mm. It is relatively longer compared with the planar patch (Lp = 25mm), thus making possible interference easy to happen. The ranges of the tilting and orientation angles are given as [0°, 60°] and [0°, 360°], respectively.

First, the whole surface was sampled into a set of discrete points. The cylindrical patch is classified as interference-prone, while most of the two planar patches are interference-free (see Fig. 6a). Then, a point $\mathbf{P}(0, 0, 0)$ on the cylindrical patch was chosen for finding its accessible posture range. A set of values of orientation angle θ were obtained by uniformly sampling the range [0°, 360°] in order to obtain the complete accessible posture range of the cutter. In order to check the validity of the search algorithm, the accessible posture ranges in terms of local-gouging, rear-gouging, and global-collision, were obtained separately to each θ at $\mathbf{P}$. The results are shown in Fig. 7. It can be seen that lower-bound of λ for local-gouging, lower-bound for rear-gouging and upper-bound of λ for collision are symmetric to $\theta = 180°$. This is understandable since the composite surface is symmetric to the bottom line of the cylindrical patch.
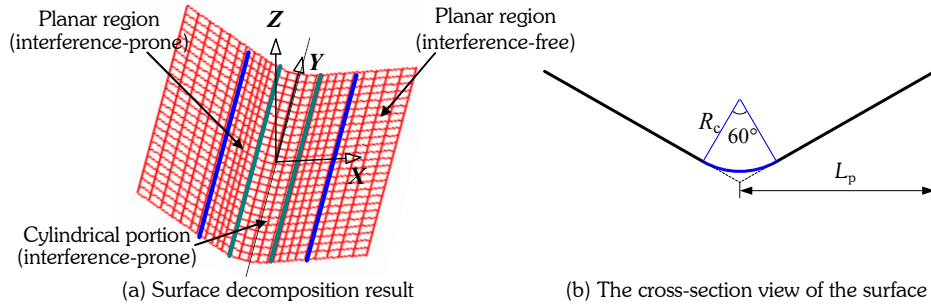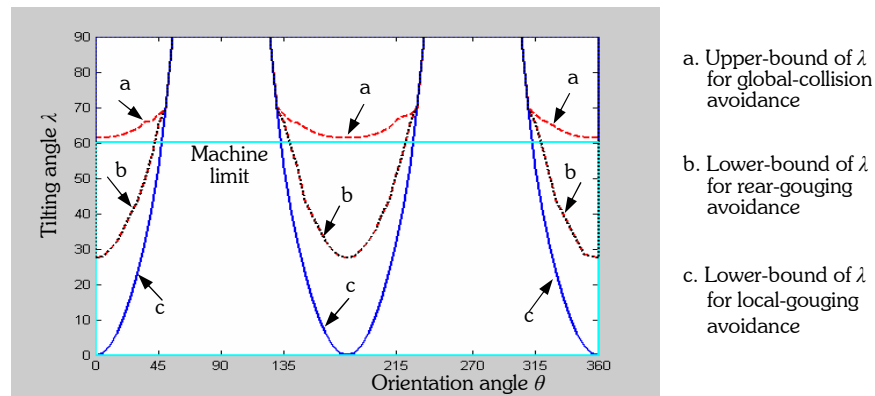
(a) Surface decomposition result   (b) The cross-section view of the surface

Fig. 6. A simple composite surface

a. Upper-bound of λ for global-collision avoidance

b. Lower-bound of λ for rear-gouging avoidance

c. Lower-bound of λ for local-gouging avoidance

Fig. 7. The accessible posture range of the cutter (R= 8mm) at **P**(0.0,0.0,0.0)

To check the validity of the results shown in Fig. 7, we calculated the exact results by taking advantage of the known geometry. The comparison between the exact results and the obtained results are given as follows:

(1) Local-gouging avoidance. We know that the curvature radius of one curve through any point on the symmetric line on the cylindrical patch is $R_c/sin^2\theta$ in any direction θ (the angle from symmetric line). The curvature radius of the cutting edge in normal direction is $R/sin\lambda$. Therefore, the minimum λ that causes no local-gouging should satisfy $R_c/sin^2\theta \geq R/sin\lambda$. We can obtain the following relation $\lambda \geq R\ sin^2\theta/R_c$. The maximum value occurs at $\theta = 52.2388°$, $127.7612°$, $232.2388°$ and $307.7612°$, which is exactly the same as that shown in Fig. 7.

(2) Rear-gouging avoidance. In this case, when λ increases (from 0°), rear-gouging between the cutter and the planar patches happens after rear-gouging between the cutter and the cylindrical patch. On the other hand, the gouging of cutting edge with the surface occurs after that of cutter bottom circular plane with the surface. Therefore, we can obtain the posture range for rear-gouging avoidance by considering only the cutting edge and the planar patches. By using geometric analysis, we obtained $\lambda_{rg-0°}= 27.5994°$. This is extremely close to the lower-bound of λ found using the search algorithm. On the other hand, the theoretical ones for other θ are also close to but slightly greater than the lower-bounds of λ found, with maximum 0.69% deviation. The reason is that only a limited number of discrete points on the spherical patch are considered for each θ and the point that results in the smallest posture range for rear-gouging avoidance may not be included in the search.

(3) Global-collision avoidance. In this case, we obtain the posture range for collision avoidance by considering only the planar patches. When λ with the value of the lower-bound of λ for rear gouging, no collision occurs. We treat this as the lower-bound of λ for collision avoidance and only need to obtain the upper-bound of λ (λ_{gc}) when collision starts occurring. On the other hand, the relatively smaller planar patches make the upper-bound of λ (λ_{gc}) for global-collision occurs between the cutter shaft surface and the surface border. By using geometric analysis, we obtained $\lambda_{gc-0°} = \lambda_{gc-180°} = 61.3466°$. These two upper-bounds are also extremely close

to the two found using the search algorithm. For other θ values, the theoretical ones are slightly less than their corresponding ones found using the algorithm, with maximum 0.15% deviation. The reason is also that only a limited number of discrete points are considered.

Based on the comparison, we can conclude that the search algorithm can effectively found the interference-free posture range for a cutter at a point on a surface. Since only a limited number of discrete points on the surface are considered in the search, the posture ranges for rear-gouging avoidance and global-collision avoidance may be slightly larger than the exact ones. This kind of error, however, could be alleviated by using high density sampling strategy.

In the second example, we show that the point-based algorithm to check the accessibility of a cutter can be easily used for cutter selection for machining a given surface. The part surface is shown in Fig. 1. The peaks and valleys of doubly curved surface are exaggerated to test robustness of the algorithm. In the surface, there is an altitude change of 58.5 mm over a linear distance of just 29.8 mm from the apex of a peak to the nadir of the closest valley. The flat-end cutters to be used for optimal cutters selection for finish machining of the surface include (R, L)=(12, 120), (10, 100), (8, 90) and (6, 80).

We took the surface point classification result from Fig. 1a, where the 201×201 points were classified into concave, convex, and saddle. Then, we took the cutter with the largest R, (12mm), in this case, to check whether it is accessible at all the points. If this cutter is not feasible, the next cutter in the list, e.g., R(8mm), is taken for the same checking procedure. This process is repeated until a feasible cutter is found. In this case, the cutter with R(6mm) is found to be the largest cutter that has accessible posture ranges at every interference-prone point. It took about 1.5 minutes of CPU time on a 2.8MHz PC to finish the checking for the cutter with R(6mm).

5. CONCLUSION

This paper introduced a comprehensive method for identifying the accessible posture range, in terms of titling and orientation angles, for a given flat-end cutter at a point on a sculptured surface in 5-axis milling. The accessible posture range is obtained by simultaneously considering machine axis limits, local-gouging, rear-gouging, and global-collision. To alleviate the extensive computation in the search process, instead of checking possible interference between the cutter and the entire part surface, a surface decomposition method is developed to divide the surface into the interference-free and interference-prone regions. This point-based accessibility analysis method can be used for determining whether a cutter is able to finish the entire surface by identifying its accessible posture range at every interference-prone point. Since the feeding direction is not considered in the search for the accessible posture range at any point, the method can be used for cutter selection before the tool-path pattern is selected. This property of the developed method offers full flexibility for tool-path pattern selection. Furthermore, it could help determine the optimal cutter postures, by imposing various optimization criteria, in the subsequent tool-path generation.

6. REFERENCES

[1]   Jensen C. G., Red W. E. and Pi J., Tool selection for five-axis curvature matched machining, *Computer-Aided Design*, Vol. 34, No. 3, 2002, pp. 251-266.
[2]   Lee Y.S. and Chang, T.C., Automatic cutter selection for 5-axis sculptured surface machining, *International Journal of Production Research*, Vol. 34, No. 4, 1996, pp. 977-998.
[3]   Li S. X. and Jerald R. B., 5-axis machining of sculptured surfaces with a flat-end cutter, *Computer-Aided Design*, Vol. 26, No. 3, 1994, pp. 165-179.
[4]   O'Neil B. *Elementary differential geometry*, Academic Press, New York, 1966.
[5]   Piegl L and Tiller W., *The NURBS Book*, Spinger-Verlag, Berlin, 1995.
[6]   Smith TS, Farouki RT. Gauss map computation for free-form surfaces, *Computer Aided Geometric Design*, Vol.18, No. 9 , 2001, pp. 831-850.
[7]   Xu X. J., Bradley C., Zhang Y. F., Loh H. T. and Wong Y. S., Tool-path generation for five-axis machining of free-form surfaces based on accessibility analysis. *International Journal of Production Research*, Vol. 40, No. 14, 2002, pp. 3253-3274.